LHB: HYDROSCIENCE JOURNAL
2022, VOL. 108, 2098069
https://doi.org/10.1080/27678490.2022.2098069

Eutrophication, oxygen status and nutrient fluxes in a macrotidal estuarine reservoir: the case of the Ria Penfeld, Bay of Brest

S. P. H. Jaffrès[a], E. Kerebel[a], M. M. Le Bagousse[a], C. J. Lefort[a], C. J. Y. Morisseau[a], K. Rouanet[a], N. C. Pemartin[a], P. Sanlis[a], J. Devesa[a,b], J.-F. Maguer[a,b] and M. Waeles[a,b]

[a]IUEM, Univ Brest, Master "Chimie de l'Environnement Marin", Plouzané, France; [b]LEMAR, Univ Brest, CNRS, IRD, Ifremer, Plouzané, France

ABSTRACT

Excessive nutrient inputs are generally perceived to be responsible for the eutrophication of estuarine and coastal systems. Here, we show that the alteration of estuarine water circulation may be a very critical driver in the case of macrotidal systems. For this study, we intensively sampled the upstream part of the Ria Penfeld in June 2021, in a period of maximum irradiance and after a period of ~7 days of closure of the Kervallon dam gate. We observed that the physico-chemical structure of the Ria Penfeld reservoir (RPR), with very high biomass (chl-*a* values up to 120 µg L^{-1}) and anoxic conditions in the bottom, was radically different from what is usually observed in the other estuaries of the region. The very high net primary production (~1700 mg C m^{-2} d^{-1}) in the RPR was associated with an important removal of nutrients, especially phosphate, resulting in a strong nutritional imbalance (molar N:Si:P ratio of 2100:1500:1) for the water exported to the downstream estuary.

KEYWORDS

Estuary; eutrophication; dam; nutrients; primary production; oxygen

MOTS-CLÉS

estuaire ; eutrophisation ; barrage ; nutriments ; production primaire ; oxygène

Eutrophisation, niveau d'oxygène et flux de nutriments dans le réservoir estuarien de la Penfeld

RÉSUMÉ

Les apports excessifs de nutriments sont généralement considérés comme responsables de l'eutrophisation des systèmes estuariens et côtiers. Nous montrons ici que la modification de la circulation des eaux estuariennes peut être un facteur particulièrement critique dans le cas des systèmes macrotidaux. Dans cette étude, nous avons intensivement échantillonné la partie amont de la Ria Penfeld en juin 2021, dans une période d'ensoleillement maximal et après une période de ~7 jours de fermeture des vannes du barrage de Kervallon. Nous avons observé que la structure physico-chimique du réservoir de Ria Penfeld (RPR), avec une biomasse très élevée (chl-a jusqu'à 120 µg L-1) et des conditions anoxiques dans le fond, était radicalement différente de ce qui est habituellement observé dans les autres estuaires de la région. La production primaire nette très élevée (~1700 mg C m^{-2} d^{-1}) était associée à une importante utilisation des nutriments, en particulier du phosphate, ce qui a entraîné un fort déséquilibre nutritionnel (rapport molaire N:Si:P de 2100:1500:1) pour l'eau exportée vers l'estuaire en aval.

1. Introduction

Eutrophication has been defined by Nixon (1995) as "an increase in the rate of supply of organic matter to an ecosystem" from allochthonous or autochthonous sources. Such a definition emphasises eutrophication as a process rather than a trophic state and differentiates the phenomenon of eutrophication from its various causes (e.g. nutrient enrichment, reductions in grazing pressure, increases in water residence time, etc.) and from its various consequences (e.g. hypoxia, fish kills, turbidity). This definition has the advantage of encompassing various situations of disruption of aquatic ecosystems. Among various causes, the excessive production of planktonic or macrophytic algae in river, estuarine and coastal environments is generally linked to an excess of nutrients (Andersen et al., 2006). This is particularly the case in Europe, whose rivers have experienced a strong increase in nitrogen (N) and phosphorus (P) levels during the twentieth century. Since the 1990s, measures applied to reduce nutrient levels in European rivers have mainly resulted in a significant reduction of P. If this effort has been successful in reducing phytoplankton biomass in some freshwater ecosystems, the same does not apply to coastal and estuarine ecosystems, where primary production is generally limited by N (Ratmaya et al., 2019).

Numerous artificial barriers have been built for energy, flood control and irrigation on the world's rivers and streams. In Europe, which has the most fragmented river network in the world, the number of artificial barriers has recently been estimated at more

CONTACT M. Waeles waeles@univ-brest.fr
Supplemental data for this article can be accessed online here: https://doi.org/10.1080/27678490.2022.2098069.

than 1.2 million (Belletti et al., 2020). A very large number of studies has been devoted to the consequences of the disturbances due to dam constructions with important changes for the waters in the immediate upstream of the dam (reservoirs) or for downstream waters. Among the various consequences observed, one can cite (1) modifications in the transport of sediments (Cunha et al., 2014; Vörösmarty et al., 2003); (2) changes in water quality, channel dynamics and morphology (Wang et al., 2018; Winton et al., 2019); and (3) disturbances in the migration and dispersal of aquatic organisms (Reid et al., 2019; Thieme et al., 2020). In reservoirs, warming of the surface waters generally induces stratification and thus facilitates the start of a spring phytoplankton bloom by maintaining plant cells in a layer a few metres below the surface, well exposed to light and rich in nutrients (Pinay et al., 2017). Dam construction can also alter nutrient fluxes along the land-ocean continuum as a result of biogeochemical processes in reservoirs (Teodoru & Wehrli, 2005; Van Cappellen & Maavara, 2016). Both changes in riverine nutrient fluxes and modifications in nutrient ratios related to damming can have multiple ecological impacts in the coastal zone, notably on community structure, as already reported, for example, for several African systems (Snoussi et al., 2007), for the coastal waters under influence of the Romaine River in Canada (Senneville et al., 2018) or for the Black Sea in the case of the Danube River (Humborg et al., 1997).

The construction of dams is not only specific to rivers but can also concern estuaries. In such systems, various reasons can lead to the construction of artificial barriers: port locks in areas with high tidal ranges, creation of recreational areas, seawalls for preventing damage from floods and tsunamis, etc. The modification of estuarine circulation that results from the presence of a dam, and which is strongly dependent on the mode of operation of the dam gate (Shin et al., 2019), can have important impacts on biological functioning and can potentially lead to eutrophication problems. However, this question has received little attention, with the notable exception of some studies conducted in different Korean estuarine systems. In the Geum estuarine reservoir, Jeong et al. (2014) showed that surface waters became much less turbid after dam construction and a strong increase of biomass was observed, with annual mean

Chl-*a* values passing from 2 to 37 μg L^{-1}. In the Yeongsan estuarine reservoir, Lee et al. (2010), reported the occurrence of saline or thermal stratifications in some seasons which cause the development of relatively high biomass (Chl-*a* values up to 25 μg L^{-1}) and temporary hypoxic conditions at the bottom.

In the present study, we describe for the first time the vertical and longitudinal distribution of master physico-chemical and biological variables in the Ria Penfeld estuarine reservoir (Brittany, France). This reservoir, created for recreational purposes, is managed in a unique way with a flush out and refill being regularly carried out at night during spring tides and occasionally during neap tides. During these 12-h periods of gate opening, the reservoir retrieves some of its estuarine characteristics with a flood tide corresponding to the flush out of the reservoir and an ebb tide that allows the refill of the reservoir.

As part of a field project conducted during our master's degree studies, we intensively sampled this system during two days in June 2021 (14 and 15 June), during a period of maximum irradiance and after a period of ~7 days of dam gate closure. Beyond the spatial description of the system, our objectives were also to examine the oxygen status, to assess the net primary production (NPP) and to estimate the fluxes of nutrients transiting in this system.

2. Material and methods

2.1. Study area

The Penfeld River, discharging into the Bay of Brest, is 15.9 km long and has a drainage basin of 64 km^2 and an average water discharge of 0.69 m^3 s^{-1}. It collects waters from a poorly industrialised catchment with agricultural areas, urban areas and meadows representing the majority of the soil occupancy. The Ria Penfeld (estuary), situated within the city of Brest, expands from Penfeld street (km 0, 48.409°N, 4.525° W) to Brest military harbour (km 5, 48.378°N, 4.494° W) covering a distance of ~5.0 km (Figure 1). The Kervallon Dam (km 2.2, 48.395°N, −4.510°W) was built in 1987 to create a recreational area, called "les rives de Penfeld", on the banks of the upstream part of the Ria Penfeld. This upstream part of the Ria, corresponding to the Ria Penfeld Reservoir (RPR), is our studied system. It is worth mentioning that the gate of Kervallon Dam is regularly open at spring tides (i.e. tidal range above 5 m) during the ebb tide of the night and occasionally during the neap tide period allowing the release of all water above 4.2 m relative to the lowest low tide of the Bay of Brest (rlt). The RPR is then refilled during the following flood tide with a mixture of brackish/marine waters from the downstream estuary. Supplemental Figure S1 displays the water level in the Bay of Brest and within the RPR over the period preceding our sampling campaign. It shows that the last opening of the dam happened during the night of 7–8 June 2021, corresponding to a closure period of ~7 days before our survey, which was undertaken on 14 and 15 June 2021. During our survey, the water level was 6.5 m rlt and the different depths given in our study were thus measured relative to this level. When filled, the RPR (2.2 km long) has an average depth of ~5 m and a surface area of 0.12 km^2,

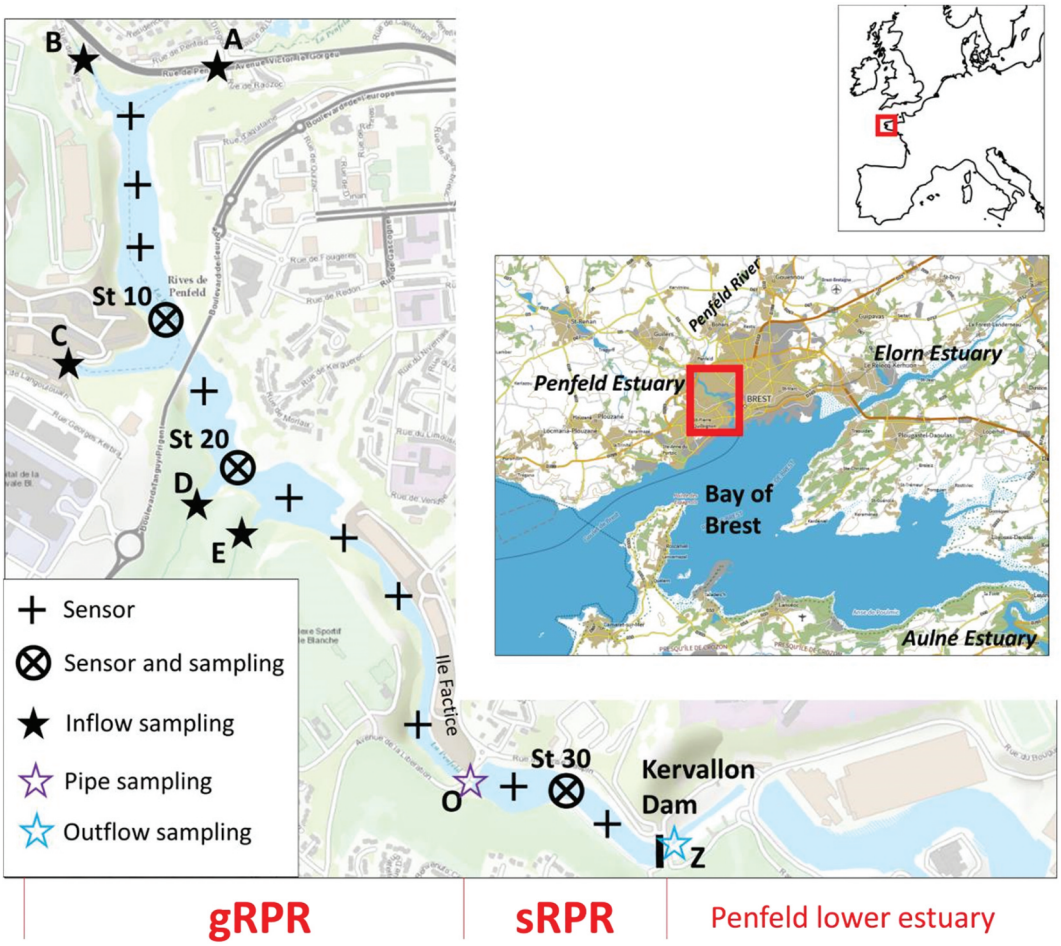

Figure 1. Study area and sampling stations along the Ria Penfeld reservoir; gRPR and sRPR correspond to the great Ria Penfeld reservoir and the small Ria Penfeld reservoir, respectively. A, B, C, D, E, O and Z correspond to the sampling at the different tributaries and outlets; crosses correspond to stations were temperature, salinity and dissolved oxygen profles were realised; St 10, St 20 and St 30 correspond to the sampling stations were water samples were collected at different depths.

representing a volume of ~600,000 m^3. Different embankments have been built on the RPR (see Figure 1) over different periods, with one of them connecting the two banks at km 1.7 and separating the RPR into two parts, which will be referred to as great RPR (gRPR) and small RPR (sRPR), respectively. These two parts of the RPR are interconnected by two pipes ~40 m long and 3 m in diameter, with the bottom situated at 4.1 m rlt. During our sampling, the bottoms of the pipes were situated at a depth of 1.4 m allowing a free overflow of this layer between the gRPR and the sRPR.

The riverine waters filling the RPR come mainly from the Penfeld River (A) but also from other tributaries situated on the western bank of the gRPR (B, C, D and E). All of these streams, located on the urban periphery, drain a mixture of wooded, agricultural and urbanised areas, with the agricultural influence being more pronounced for streams A and B. During our study, the discharge of the different tributaries (at points A, B, C, D and E; see Figure 1), estimated using a using an FP111 flow probe (Global Water), were 0.5, 0.3, 0.3, 0.2 and 0.2 $m^3\ s^{-1}$, respectively, corresponding to a total inflow of 1.5 $m^3\ s^{-1}$. This inflow creates a circulation of low-salinity waters on top of the RPR. The upper layer of low-salinity waters had a thickness of ~1.8 m during our survey (see Figure 2) and the estimated renewal time for this upper layer was ~2 days. As the water level of the RPR was stable during our sampling period (Supplemental Figure S1), we considered that the outflow of water from the RPR (and between the gRPR and the sRPR) was equivalent to the total inflow (i.e. 1.5 $m^3\ s^{-1}$).

2.2. On-site measurements, sampling and filtration

Temperature, salinity and dissolved oxygen profiles were performed from surface to floor at 10 stations of the gRPR and at three stations of the sRPR with probes handled from an inflatable boat. Temperature and salinity were measured with a Hanna® HI 9828 probe calibrated with a 0.1 M KCl solution. Depth and dissolved oxygen were obtained with an AP-2000 Aquaread probe calibrated at 100% and 0% saturation of dissolved

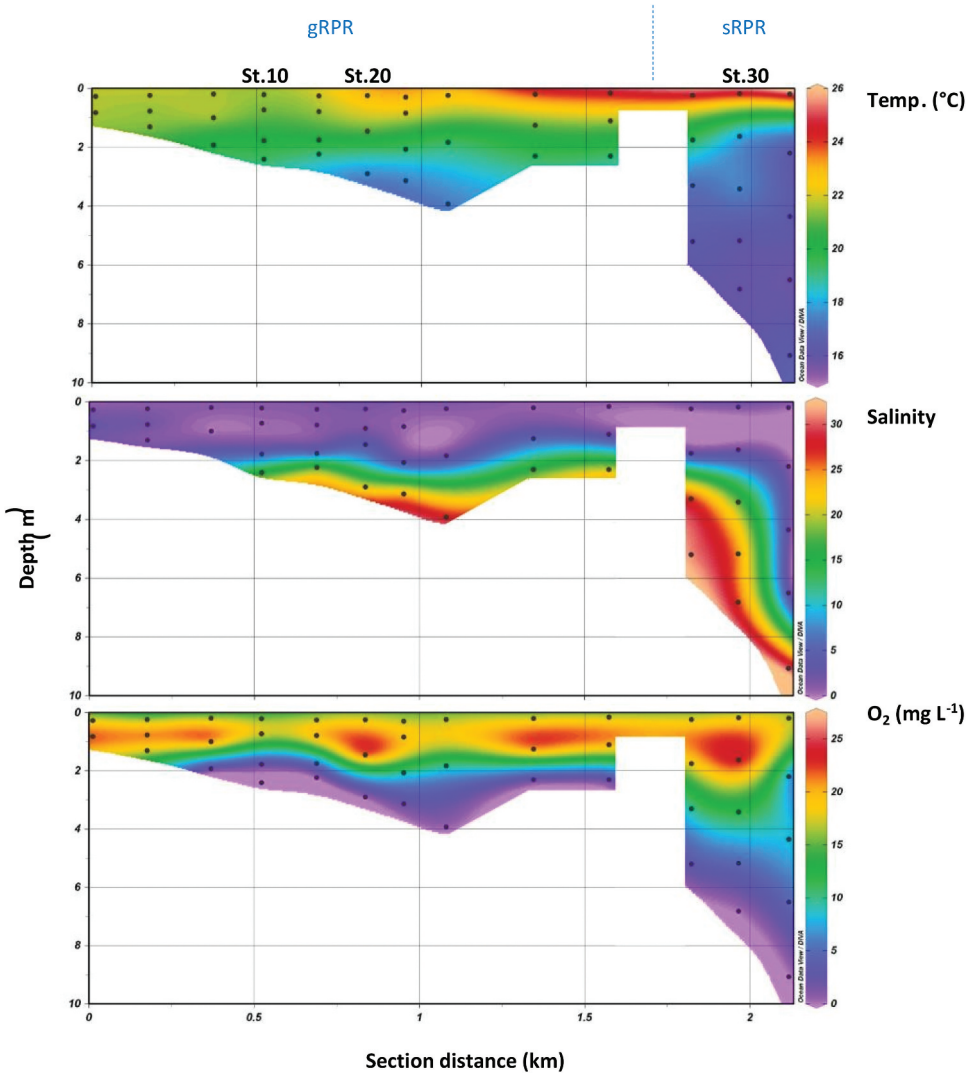

Figure 2. Distribution of temperature, salinity and dissolved oxygen along the Ria Penfeld Reservoir (RPR) in June 2021. The left side of each panel corresponds to the great RPR and the right side corresponds to the small RPR. The three panels were drawn with the Ocean Data View software using triangular mesh gridding.

oxygen. Additionnal measurements of temperature, salinity and dissolved oxygen at 1 m above the bottom of the gRPR (Station 20) were performed over the 9–15 June 2022 period. These measurements were done with a STPS10-SI from NKE and a miniDO$_2$T Logger from PME.

Water samples were collected with a 5-L Niskin bottle adapted to horizontal sampling and handled from an inflatable paddle board at various depths in the RPR (four depths at stations 10 and 20 and five depths at station 30). These water samples were transferred in 1-L HDPE bottles and filtered on-site within 1 h after sampling. Water samples were also collected by hand with 1-L HDPE bottles in (1) the different tributaries (points A, B, C and E; note that point D, within a military area, was not accessible); (2) at the outlet of the pipe connecting the gRPR and the sRPR (point O); and (3) at the final outlet of the RPR at the Kervallon Dam (point Z). These water samples were also filtered on-site within 1 h after sampling.

Whatman filters (0.7-µm GF/F) were used to collect and measure particulate organic carbon (POC), chlorophyll-a (Chl-*a*) and phaeopigments. The filters used for POC, as well as the glass container for the storage of POC filters, were previously ignited at 450°C for 4 h. The filtrates were transferred into 125-mL HDPE flasks and were used for nutrient measurements (nitrate, phosphate and orthosilicic acid). After filtration, filters and filtrates were immediately stored in an icebox (0–4°C) and then at 20°C (until analyses) in the home lab at the end of the day. Prior to use, all the items employed for sampling, filtration and storage of filtrates were thoroughly rinsed with deionised water.

2.3. Measurements

Nitrate and orthosilicic acid were analysed by colorimetry on a Bran + Luebbe AutoAnalyzer 3 with a precision of 0.03 µM (Strickland & Parsons, 1972). Before analysis, samples were diluted by 5 to 25 (for depth and surface waters, respectively) in

order to fit within the calibration ranges. Phosphate concentrations were determined using the Murphy and Riley (1962) method (0.02 µM precision). POC was determined according to the Johnson (1949) method standardised with a glucose solution. Organic compounds were oxidised with dichromate ions in a sulphochromic solution. The excess dicromate was then quantified with an 0.100 M Fe(II) solution. Chl-*a* and phaeopigments were extracted with an acetone–water mixture (90/10, v/v) and measured by the Lorenzen (1967) method with an 8% precision on Turner fluorometer. Gross primary production (GPP) and NPP were determined as follows. Incubation of waters over a 24-h period was done at stations 20 and 30. In each case oxygen-saturated water from the surface was distributed in dark (125-mL) and clear (1-L) Winkler flasks. The different flask couples (dark/clear) were then attached to a net and incubated at different depths for 24 h. Within 10 min after recovery, manganese chloride (3 M) and alkaline-iodide (NaOH 8 M, NaI 4 M) solutions were added in each flask for dissolved-oxygen determination. Samples were then analysed the following day at the home laboratory by the spectrophotometric Winkler method of Labasque et al. (2004) (precision <1%) using a sulphuric acid solution (10 M) and a potassium iodate (5.95 M) solution for standard preparations. Oxygen was then converted to carbon assuming a molar photosynthetic quotient of 1.0 (Robinson, 2008).

3. Results

Figure 2 describes the vertical distribution of temperature, salinity and dissolved oxygen across the RPR. For both parts of the reservoir (gRPR and sRPR) a strong thermohaline stratification of the water column was observed. The surface layer (0–1.8 m) was characterised by warm temperatures (range 20–26°C) and low salinities (range 0–10). This surface layer was also well-oxygenated, with dissolved oxygen concentrations ranging from 15 to 25 mg L^{-1}, corresponding to oxygen saturation values in the range of 180–300%. Conversely, the bottom layer of the reservoir was characterised by colder temperatures (range 16–20°C), higher salinities (10–30) and oxygen concentrations lower than 10 mg L^{-1}. It is worth noting that anoxic conditions were encountered in both the gRPR and the sRPR, at the bottom of the water column.

The vertical distribution of nutrients is given in Figure 3. Relatively closed distributions were observed for each nutrient at each station of the RPR. For nitrate and orthosilicic acid (Figure 3(a,b)), high concentrations were observed close to the surface (range 350–400 µM and 250–300 µM, respectively) with decreasing values reaching 50–100 µM towards the bottom of each station. For phosphate, concentrations in the range of 0.1–0.2 µM were generally observed over the whole water column, and a strong increase was found at the bottom with values above 0.6 µM in the gRPR (stations 10 and 20), and over 1.0 µM in the sRPR (station 30). It is also worth noting that (1) slightly higher nutrient concentrations were observed at the surface at station 10 compared to other stations and (2) slightly higher concentrations of nitrate and orthosilicic acid were observed just below the surface (at ~1 m) at stations 10 and 20. Nutrient–salinity distributions (Figure 4) show that the nutrient concentrations in the RPR were situated between those of the fluvial source (~400, ~300 and ~1.8 µM for nitrate, orthosilicic acid and phosphate, respectively) and those of the Bay of Brest (0.06, 1.3 and 0.07 µM, respectively). These distributions also evidenced non-conservative distributions with significant deviations from linearity for the samples collected in the subsurface layer (0–2 m), which should be related to the consumption of these nutrients by the plankton community.

The distribution of Chl-*a* (Figure 3(d)) indicates the occurrence of very high algal biomass close to the surface over the RPR with concentrations in the range of 60–80 µg L^{-1} at 0–1 m for each station and close to 100–120 µg L^{-1} at 2 m for stations 20 and 30. At greater depths, the observed Chl-*a* concentrations were lower (range 10–30 µg L^{-1}) but still indicated a significant amount of algal biomass. As for Chl-*a*, very high POC concentrations were found in the RPR (Figure 3(e)) with values in the range of 4000–7000 µg L^{-1}. It is worth noting here that the highest concentrations (i.e. above 6000 µg L^{-1}) were found at ~2 m at stations 10 and 20 and along the whole water column in the sRPR (station 30). The POC:Chl-*a* ratio, which can be considered an indicator of POC of algal origin, shows a very marked and relatively similar distribution for each station (Figure 3(f)), with values close to 50 near the surface (0–2 m) and values above 200 below 2 m.

4. Discussion

The presence of the dam in the Penfeld estuary leads to a physico-chemical structure that is radically different from that observed in the other estuaries of the region (Bassoulet, 1979), within the Bay of Brest (Del Amo et al., 1997; Le Pape et al., 1996) and more generally in macrotidal estuarine coastal systems (Allen et al., 1980). Usually, very homogeneous or weakly stratified conditions are observed in these systems. The energy provided by the tide allows efficient vertical mixing. Thus, the differences in temperature and salinity between surface and

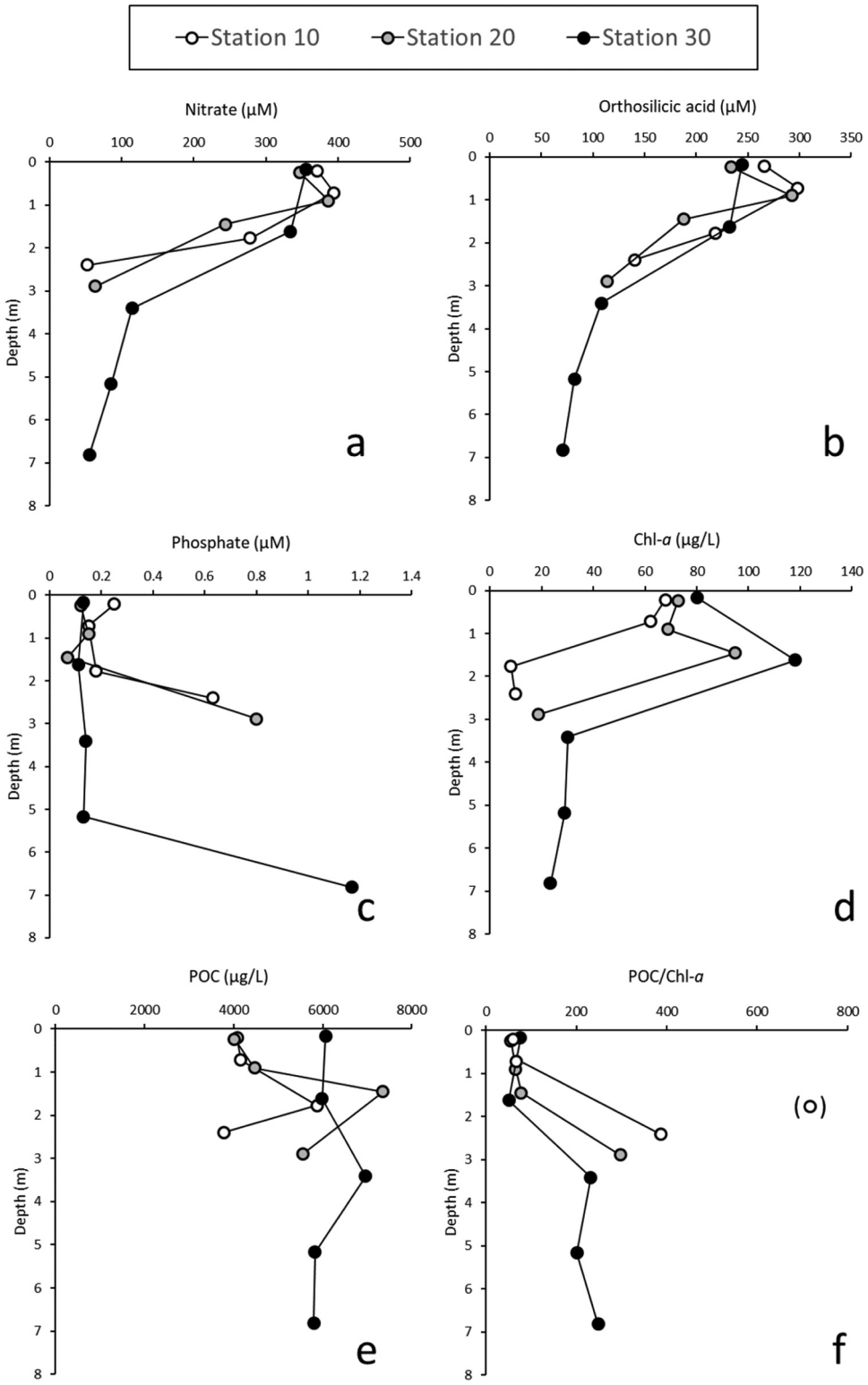

Figure 3. Vertical distributions of (a) nitrate, (b) orthosilicic acid, (c) phosphate, (d) chlorophyll-*a* (Chl-*a*), (e) particulate organic carbon (POC) and (f) POC:Chl-*a* ratio at stations 10, 20 and 30 in the Ria Penfeld reservoir in June 2021.

bottom waters are generally small. Indeed, our CTD (Conductivity Temperature Depth) profiles performed in the Aulne and Elorn estuaries under different tidal conditions indicated that vertical gradients of temperature and salinity do not exceed 1°C and 5 salinity units, respectively. The efficient vertical mixing due to the tide also allows good oxygenation of the entire estuary. Even if oxygen deficits can appear in the areas of maximum turbidity of these systems in summer, especially in systems disturbed by agricultural activities and therefore subject to significant inputs of nutrients and organic matter, a generalised anoxia, as observed in the Ria Penfeld (Figure 2), has been very rarely reported. Indeed, the only estuary in the Brittany region to have reached the stage of lethal anoxia is the Bay of

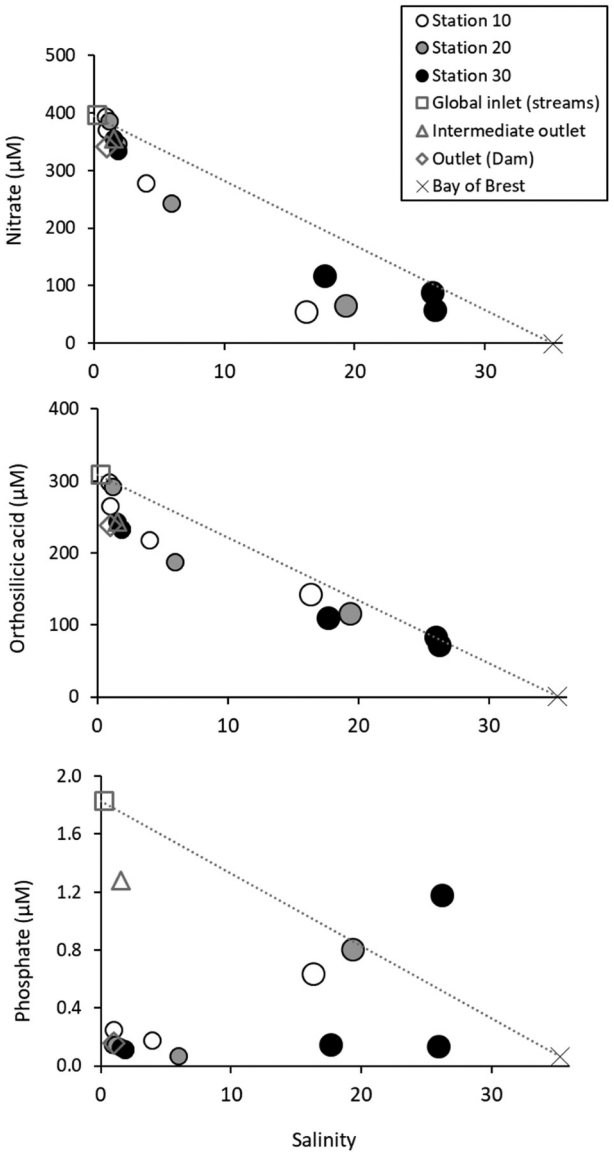

Figure 4. Concentrations of nitrate, orthosilicic acid and phosphate as a function of salinity in the RPR in June 2021. Global inlet concentrations correspond to flowweighted mean concentration of the different tributaries. Marine end-member concentrations (Bay of Brest) were deduced from simultaneous measurements at the nearby SOMLIT (Service d'Observation en Milieu Littoral) marine station (Rimmelin-Maury et al., 2016). Note that samples collected at depths below 2 m (for stations 10, 20 and 30) are described with larger circles than the samples collected within the subsurface layer (0–2 m).

Vilaine, where a massive mortality of fish and benthic invertebrates occurred in July 1982 (Menesguen et al., 2001).

The anoxia observed in the deep waters of the Ria Penfeld is directly related to the presence of the dam and its insufficiently frequent opening. The addition of brackish water during the spring tide periods (tidal range above 5 m) and the subsequent closure of the dam during neap tides leads to the establishment of a strong haline stratification. This will allow a flow of nutrient-rich water of a strongly fluvial nature at the surface and therefore favour the presence of a large biomass associated with a high primary production. It will also lead to the retention of salty water at depth. Oxygen depletion in the deep waters then results from a combination of two factors: an intense bacterial activity that degrades organic matter produced in surface waters and exported to depth and very poor ventilation of the deep layer isolated under the thermo-haline stratification.

The high biomass in the RPR is highlighted by the particularly high Chl-*a* levels in the 0–2 m layer, with values ranging from 60 to 120 µg L^{-1}. The work of Monbet (1992) and Cloern and Jassby (2008) showed that macrotidal estuaries are only very rarely characterised by Chl-*a* concentrations above 10 µg L^{-1}, even for the most nutrient-rich systems. This is due to the tidal mixing, which not only makes the environment more turbid by suspending fine particles but also reduces the light available to the cells by decreasing their residence time in the euphotic zone (Demers et al., 1979). Because of modified water circulation induced by the dam, the biomass concentration in the Penfeld appears at the same amount as those of the richest estuarine systems compiled by Monbet (1992) and Cloern and Jassby (2008). In accordance with this high biomass occurrence, the POC:Chl-*a* ratios in the surface layer of the Ria Penfeld, with values in the range of 50–75, indicate that the particulate organic matter is essentially of autochthonous origin. Indeed, Abril et al. (2000) showed that POC:Chl-*a* ratios can vary over a wide range, from 40 for purely algal organic matter to values >10,000 for degraded organic matter of allochthonous origin (soil, river, etc.).

The NPP measured at stations 20 and 30 (Supplemental Figure S1) was 1700 and 1500 mg C m^{-2} d^{-1}, respectively. These values fall within the same range as those found in summer in hypertrophic systems including the Swan River estuary (Thompson, 1998), the mesohaline zone of the Chesapeake Bay (Harding et al., 2020) and the Sagami Bay (Ara & Hiromi, 2007). Differently from hypertrophic systems, in which the tidal range is low and tidal mixing is limited, it has been shown that for macrotidal systems, the light limitation imposed by the turbid and mixing conditions results in a primary production that is low and usually counterbalanced by respiration. In such macrotidal systems, the maximum NPP values along the seasonal cycle are usually under 500 mg C m^{-2} d^{-1} (Glé et al., 2008; Kocum et al., 2002).

Overall, the gate closure of the Kervallon dam prevents tidal mixing and extends the residence time of the waters in the RPR. It also causes a strong stratification of the system, which is further reinforced by the thickening of the surface layer with continuous freshwater inputs over the period of the gate closure. These inputs of fresh water rich in nutrients in the surface layer probably accentuate the primary production and

its export to depth. The setting up of this stratification also isolates the salty bottom water and allows the loss of oxygen within it. Thus, the dam is responsible not only for the eutrophication of the system but also for the abnormal anoxic conditions observed in the bottom waters. It is worth mentioning here that our study was conducted over a short period in June. Monitoring over a longer period is obviously needed to explore the representativeness of the observed conditions.

Due to the low primary production in macrotidal estuaries, nutrients are generally not used significantly, and the observed nutrient concentrations are therefore essentially the result of the efficient dilution of fluvial waters by marine waters. Thus, nutrient–salinity distributions are usually linear in the oligohaline and mesohaline zones of these systems, including those of the Bay of Brest (Delmas & Treguer, 1983). In contrast to this general rule, significant deviations from the theoretical dilution lines are observed for the Ria Penfeld (Figure 4). The strong "loss" of nutrients is very clear in the oligohaline surface waters. Indeed, at a salinity of 5, negative deviations of about 100, 70 and 1.7 µM are observed for nitrate, orthosilicic acid and phosphate, respectively. It is worth noting that the higher phosphate concentrations (> 0.6 µM) observed at salinity above 15 (Figure 4) and corresponding to anoxic bottom waters (see Figures 2 and 3) likely result from the release of phosphate caused by the reduction of a FeOOH-phosphate complex in anoxic conditions (Golterman, 2001).

Our data also allowed us to quantify the removal of the different nutrients by comparing the concentrations measured for the different inlets to those measured at the outlet (Table 1). According to our estimations, 14%, 23% and 90% of the input flux of nitrate, orthosilicic acid and phosphate, respectively, is trapped within the reservoir. Such fractions are relatively high considering the high nutrient concentrations of the fluvial waters (i.e. ~400, ~300 and ~1.8 µM, respectively). It is worth noting here that these fluvial concentrations are within the usual range observed for the other system of the area that are also impacted by agricultural practices and urbanisation. These rivers (e.g. Aulne, Elorn, Flèche, Quillimadec) display concentrations in the range of 200–600 µM for nitrate, 100–300 µM for orthosilicic acid and 0.5–3.0 µM for phosphate (Quinquis, 2018). Because of the more intense removal of phosphate in the RPR, the nutrient ratios were heavily modified. Indeed, the molar N:Si:P ratio associated with the input flux was 210:170:1, whereas the molar N:Si:P ratio associated with the output flux was 2100:1500:1.

What are the consequences of this important abatement in P and such an imbalance in nutrients for the waters located downstream of the reservoir? According to a study by Ratmaya et al. (2019), carried out in the Bay of Vilaine, a reduction in P inputs without a significant reduction in N inputs does not necessarily lead to a limitation of primary production in estuarine and coastal waters, as may be the case in fluvial systems that are P-limited. The non-limitation of P in marine ecosystems is thought to be due to a much more efficient recycling of this element due to the presence of sulphate, one of the major ions in seawater, which would reduce the efficiency of sediments in retaining P (Caraco et al., 1990).

Finally, the influence of the RPR on the coastal waters of the Bay of Brest is probably limited – on the one hand because the water flow of the Penfeld is low compared to other rivers of the catchment area (Aulne and Elorn) and on the other hand because the intense tidal currents in the Bay of Brest quickly dilute the nutrients delivered by the different rivers of the catchment (Pinay et al., 2017). However, the same cannot be said for the downstream part of the Penfeld estuary, which is under the direct influence of the spillway from the RPR and of the flush-out of the reservoir (especially after a long period of gate closure). Further investigation is needed in the downstream part of the estuary to examine the impact of the exacerbated nutritional imbalance that results from the water transit in the RPR and of the transfer of organic matter from the hypertrophied RPR.

In order to improve the situation of the Ria Penfeld regarding eutrophication, anoxic conditions and nutrient imbalance, a more frequent opening of the dam in its current functioning (with a flush-out of

Table 1. Nutrient concentrations and fluxes transiting in the RPR (Ria Penfeld Reservoir) system. Input concentrations correspond to the discharge-weighted means of the measurements in the different tributaries flowing into the RPR. Intermediate and output concentrations correspond to the measurements at the outlet of the pipe between gRPR (great Ria Penfeld Reservoir) and sRPR (small Ria Penfeld Reservoir) and at the outlet of the Kervallon dam, respectively. Fluxes were then estimated using a water discharge of 1.5 $m^3 s^{-1}$. The outflow of water from the RPR (and between the gRPR and the sRPR) was considered equivalent to the total inflow of water (i.e. 1.5 $m^3 s^{-1}$) because of the stable water level during the sampling period (see Supplemental Figure S1).

Concentrations (µM)	Nitrate	Orthosilicic acid	Phosphate	N:Si:P molar ratio
Tributaries (A–E)	395	308	1.83	210:170:1
Outlet of pipe O	372	254	1.34	280:190:1
Outlet of pipe Z	341	238	0.16	2100:1500:1
Fluxes (kg d^{-1})	**Nitrate**	**Orthosilicic acid**	**Phosphate**	
Input flux (A–E)	720	1120	7.4	
Intermediate flux (O)	670	930	5.4	
Output flux (Z)	620	870	0.64	

waters above 4 m rlt) would probably be more effective. Indeed, additional measurements were conducted over a 7-day period in June 2022 to examine the evolution of the deep-water characteristics after a renewal of the RPR (Supplemental Figure S3). These data were obtained 1 m above the bottom of the gRPR (at Station 20). Over the neap tide and gate closure period (until 12 June 2022), the deep waters became anoxic. Then, the gate opening during the three following nights under spring tides allowed a gradual reoxygenation of the deep waters of the RPR. Our future work will be conducted in closer collaboration with the system managers. We plan to examine whether more frequent opening of the Kervallon gate, i.e. day and night, and regardless of tidal conditions, would effectively improve the overall characteristics of the Ria Penfeld.

Acknowledgements

We are very grateful to ISblue for funding this educational project that involved students in the SML master's program ("Sciences de la Mer et du littoral, mention Chimie de l'environnement Marin"). We also thank the teachers who participate in the training of the master's students in related fields, Peggy Rimmelin (UMS 3113-IUEM) for the lending of sensors and Nicolas Floc'h (BMO) for providing the water level data for the RPR. A special mention to Thilo Berhends from the University of Utrecht for inspiring this educational project. The objective of this project was to design and run a teaching module covering the different aspects of research work applied to estuarine processes. Constructed collaboratively, the first step was to identify an original research question and to establish a reasonable study strategy in accordance with the students' knowledge and technical skills. The next step consisted of preparing the field study, planning the different tasks and how to carry them out both in the field and in the laboratory. In this step, student autonomy was prioritised to help them understand the difficulties related to sharing tasks and the traceability of data and experimental protocols. Following the field and lab work, a collaborative data exploitation was undertaken. The supervisor's role here was to accompany the students in their decision-making related to representing the results, and analyse the results in order to better identify the key processes involved. In the last step, the students met the challenge of submission to a peer-reviewed journal and faced the discipline and scientific rigor imposed by editorial work.

Disclosure statement

No potential conflict of interest was reported by the authors.

Data availability statement

The data that support the findings of this study are available from the corresponding author [MW].

References

Abril, G., Riou, S., Etcheber, H., Frankignoulle, M., De Wit, R., & Middelburg, J. J. (2000). Transient, tidal timescale, nitrogen transformations in an estuarine turbidity maximum—Fluid mud system (The Gironde, South-west France). *Estuarine, Coastal and Shelf Science*, *50*(5), 703–715. https://doi.org/10.1006/ecss.1999.0598

Allen, G. P., Salomon, J. C., Bassoullet, P., Du Penhoat, Y., & De Grandpre, C. (1980). Effects of tides on mixing and suspended sediment transport in macrotidal estuaries. *Sedimentary Geology*, *26*(1–3), 69–90. https://doi.org/10.1016/0037-0738(80)90006-8

Andersen, J. H., Schlüter, L., & Ærtebjerg, G. (2006). Coastal eutrophication: Recent developments in definitions and implications for monitoring strategies. *Journal of Plankton Research*, *28*(7), 621–628. https://doi.org/10.1093/plankt/fbl001

Ara, K., & Hiromi, J. (2007). Temporal variability in primary and copepod production in Sagami Bay, Japan. *Journal of Plankton Research*, *29*(suppl_1), i85–i96. https://doi.org/10.1093/plankt/fbl069

Bassoulet, P. (1979). *Etude de la dynamique des sédiments en suspension dans l'estuaire de l'Aulne (rade de Brest)*. Université de Bretagne occidentale.

Belletti, B., de Leaniz, C. G., Jones, J., Bizzi, S., Börger, L., Segura, G., Castelletti, A., Van de Bund, W., Aarestrup, K., Barry, J., Belka, K., Berkhuysen, A., Birnie-Gauvin, K., Bussettini, M., Carolli, M., Consuegra, S., Dopico, E., Feierfeil, T., Fernández, S., … Zalewski, M. (2020). More than one million barriers fragment Europe's rivers. *Nature*, *588*(7838), 436–441. https://doi.org/10.1038/s41586-020-3005-2

Caraco, N., Cole, J., & Likens, G. E. (1990). A comparison of phosphorus immobilization in sediments of freshwater and coastal marine systems. *Biogeochemistry*, *9*(3), 277–290. https://doi.org/10.1007/BF00000602

Cloern, J. E., & Jassby, A. D. (2008). Complex seasonal patterns of primary producers at the land–sea interface. *Ecology Letters*, *11*(12), 1294–1303. https://doi.org/10.1111/j.1461-0248.2008.01244.x

Cunha, D. G. F., Do Carmo Calijuri, M., & Dodds, W. K. (2014). Trends in nutrient and sediment retention in Great Plains reservoirs (USA). *Environmental Monitoring and Assessment*, *186*(2), 1143–1155. https://doi.org/10.1007/s10661-013-3445-3

Del Amo, Y., Le Pape, O., Tréguer, P., Quéguiner, B., Ménesguen, A., & Aminot, A. (1997). Impacts of high-nitrate freshwater inputs on macrotidal ecosystems. I. Seasonal evolution of nutrient limitation for the diatom-dominated phytoplankton of the Bay of Brest (France). *Marine Ecology Progress Series*, *161*, 213–224. https://doi.org/10.3354/meps161213

Delmas, R., & Treguer, P. (1983). Evolution saisonnière des nutriments dans un écosystème eutrophe d'Europe occidentale (la rade de Brest). Interactions marines et terrestres. *Oceanologica Acta*, *6*(4), 345–356. https://archimer.ifremer.fr/doc/00120/23122/20969.pdf

Demers, S., Lafleur, P., Legendre, L., & Trump, C. (1979). Short-term covariability of chlorophyll and temperature in the St. Lawrence Estuary. *Journal of the Fisheries Research Board of Canada*, *36*(5), 568–573. https://doi.org/10.1139/f79-081

Glé, C., Del Amo, Y., Sautour, B., Laborde, P., & Chardy, P. (2008). Variability of nutrients and phytoplankton primary production in a shallow macrotidal coastal

ecosystem (Arcachon Bay, France). *Estuarine, Coastal and Shelf Science*, *76*(3), 642–656. https://doi.org/10.1016/j.ecss.2007.07.043

Golterman, H. (2001). Phosphate release from anoxic sediments or What did Mortimer really write?'. *Hydrobiologia*, *450*(1), 99–106. https://doi.org/10.1023/A:1017559903404

Harding, L. W., Mallonee, M. E., Perry, E. S., Miller, W. D., Adolf, J. E., Gallegos, C. L., & Paerl, H. W. (2020). Seasonal to inter-annual variability of primary production in Chesapeake Bay: Prospects to reverse eutrophication and change trophic classification. *Scientific Reports*, *10*(1), 1–20. https://doi.org/10.1038/s41598-020-58702-3

Humborg, C., Ittekkot, V., Cociasu, A., & Bodungen, B. V. (1997). Effect of Danube River dam on Black Sea biogeochemistry and ecosystem structure. *Nature*, *386*(6623), 385–388. https://doi.org/10.1038/386385a0

Jeong, Y. H., Yang, J. S., & Park, K. (2014). Changes in water quality after the construction of an estuary dam in the geum river estuary dam system, Korea. *Journal of Coastal Research*, *30*(6), 1278–1286. https://doi.org/10.2112/JCOASTRES-D-13-00081.1

Johnson, M. J. (1949). A rapid micromethod for estimation of non-volatile organic matter. *Journal of Biological Chemistry*, *181*(2), 707–711. https://doi.org/10.1016/S0021-9258(18)56593-5

Kocum, E., Underwood, G. J., & Nedwell, D. B. (2002). Simultaneous measurement of phytoplanktonic primary production, nutrient and light availability along a turbid, eutrophic UK east coast estuary (the Colne Estuary). *Marine Ecology Progress Series*, *231*, 1–12. https://doi.org/10.3354/meps231001

Labasque, T., Chaumery, C., Aminot, A., & Kergoat, G. (2004). Spectrophotometric Winkler determination of dissolved oxygen: Re-examination of critical factors and reliability. *Marine Chemistry*, *88*(1–2), 53–60. https://doi.org/10.1016/j.marchem.2004.03.004

Le Pape, O., Del Amo, Y., Menesguen, A., Aminot, A., Quequiner, B., & Treguer, P. (1996). Resistance of a coastal ecosystem to increasing eutrophic conditions: The Bay of Brest (France), a semi-enclosed zone of *Western Europe*. *Continental Shelf Research*, *16*(15), 1885–1907. https://doi.org/10.1016/0278-4343(95)00068-2

Lee, Y. G., Kang, J.-H., Ki, S. J., Cha, S. M., Cho, K. H., Lee, Y. S., Park, Y., Lee, S. W., & Kim, J. H. (2010). Factors dominating stratification cycle and seasonal water quality variation in a Korean estuarine reservoir. *Journal of Environmental Monitoring*, *12*(5), 1072–1081. https://doi.org/10.1039/b920235h

Lorenzen, C. J. (1967). Determination of Chlorophyll and Pheo-Pigments: Spectrophotometric Equations. *Limnology and oceanography*, *12*, 343–346. doi:10.4319/lo.1967.12.2.0343

Menesguen, A., Aminot, A., Belin, C., Chapelle, A., Guillaud, J.-F., Joanny, M., Lefebvre, A., Merceron, M., Piriou, J.-Y., & Souchu, P. (2001). *L'eutrophisation des eaux marines et saumâtres en Europe, en particulier en France* (Ifremer).

Monbet, Y. (1992). Control of phytoplankton biomass in estuaries: A comparative analysis of microtidal and macrotidal estuaries. *Estuaries*, *15*(4), 563–571. https://doi.org/10.2307/1352398

Murphy, J., & Riley, J. P. (1962). A modified single solution method for the determination of phosphate in natural waters. *Analytica Chimica Acta*, *27*, 31. https://doi.org/10.1016/S0003-2670(00)88444-5

Nixon, S. W. (1995). Coastal marine eutrophication: A definition, social causes, and future concerns. *Ophelia*, *41*(1), 199–219.36. https://doi.org/10.1080/00785236.1995.10422044

Pinay, G., Gascuel, C., Menesguen, A., Souchon, Y., Le Moal, M., Aissani, L., Anschutz, P., Barthélemy, C., Béline, F., & Bornette, G. (2017). *Restitution de l'ESCo Eutrophisation. Manifestations, causes, conséquences et prédictibilité*, CNRS - Ifremer - INRA - Irstea (France),144 pages.

Quinquis, Y. (2018). *Analyse des sels nutritifs présents dans les rivières Finistériennes*.IUEM. https://www-iuem.univ-brest.fr/ecoflux/productions-scientifiques/bilansannuels-ecoflux/Rapport_Ecoflux_Yasmine_Quinquis.pdf

Ratmaya, W., Soudant, D., Salmon-Monviola, J., Plus, M., Cochennec-Laureau, N., Goubert, E., Andrieux-Loyer, F., Barille, L., & Souchu, P. (2019). Reduced phosphorus loads from the Loire and Vilaine rivers were accompanied by increasing eutrophication in the Vilaine Bay (south Brittany, France). *Biogeosciences*, *16*(6), 1361–1380. https://doi.org/10.5194/bg-16-1361-2019

Reid, A. J., Carlson, A. K., Creed, I. F., Eliason, E. J., Gell, P. A., Johnson, P. T., Kidd, K. A., MacCormack, T. J., Olden, J. D., Ormerod, S. J., Smol, J. P., Taylor, W. W., Tockner, K., Vermaire, J. C., Dudgeon, D., & Cooke, S. J. (2019). Emerging threats and persistent conservation challenges for freshwater biodiversity. *Biological Reviews*, *94*(3), 849–873. https://doi.org/10.1111/brv.12480

Rimmelin-Maury, P., l'Helguen, S., Répécaud, M., Quéméner, L., Beaumont, L., Grossteffan, E., Jolivet, A., Chauvaud, L., Tréguer, P., & Bozec, Y. (2016). *MAREL-Iroise/SOMLIT-Brest: Un outil à" fonctions-multiples", pour l'observation des eaux côtières*. In François G., Schmitt, Alain, Lefebvre. Mesures à haute résolution dans l'environnement marin côtier CNRS Editionspp.31- 39.

Robinson, C. (2008). *Heterotrophic bacterial respiration*, In DL., Kirchman(Ed.). Microbial Ecology of the Oceans, Vol. 2nd edition, pp. 299–334, Wiley.

Senneville, S., Schloss, I. R., Drouin, S. S. O., Bélanger, S., Winkler, G., Dumont, D., Johnston, P., & St-Onge, I. (2018). Moderate effect of damming the Romaine River (Quebec, Canada) on coastal plankton dynamics. *Estuarine, Coastal and Shelf Science*, *203*, 29–43. https://doi.org/10.1016/j.ecss.2018.02.006

Shin, H.-J., Lee, G., Kang, K., & Park, K. (2019). Shift of estuarine type in altered estuaries. *Anthropocene Coasts*, *2*(1), 145–170. https://doi.org/10.1139/anc-2018-0013

Snoussi, M., Kitheka, J., Shaghude, Y., Kane, A., Arthurton, R., Tissier, M. L., & Virji, H. (2007). Downstream and coastal impacts of damming and water abstraction in Africa. *Environmental Management*, *39*(5), 587–600. https://doi.org/10.1007/s00267-004-0369-2

Strickland, J. D. H., & Parsons, T. R. (1972). *A practical handbook of seawater analysis*. Fisheries Research Board of Canada.

Teodoru, C., & Wehrli, B. (2005). Retention of sediments and nutrients in the iron gate I Reservoir on the Danube River. *Biogeochemistry*, *76*(3), 539–565. https://doi.org/10.1007/s10533-005-0230-6

Thieme, M. L., Khrystenko, D., Qin, S., Golden Kroner, R. E., Lehner, B., Pack, S., Tockner, K., Zarfl, C., Shahbol, N., & Mascia, M. B. (2020). Dams and protected areas: Quantifying the spatial and temporal extent of global dam construction within protected areas. *Conservation Letters*, *13*(4), e12719. https://doi.org/10.1111/conl.12719

Thompson, P. A. (1998). Spatial and temporal patterns of factors influencing phytoplankton in a salt wedge estuary, the Swan River, Western Australia. *Estuaries*, *21*(4), 801–817. https://doi.org/10.2307/1353282

Van Cappellen, P., & Maavara, T. (2016). Rivers in the Anthropocene: Global scale modifications of riverine nutrient fluxes by damming. *Ecohydrology & Hydrobiology*, *16*(2), 106–111. https://doi.org/10.1016/j.ecohyd.2016.04.001

Vörösmarty, C. J., Meybeck, M., Fekete, B., Sharma, K., Green, P., & Syvitski, J. P. (2003). Anthropogenic sediment retention: Major global impact from registered river impoundments. *Global and Planetary Change*, *39* (1–2), 169–190. https://doi.org/10.1016/S0921-8181(03)00023-7

Wang, Y., Rhoads, B. L., Wang, D., Wu, J., & Zhang, X. (2018). Impacts of large dams on the complexity of suspended sediment dynamics in the Yangtze River. *Journal of Hydrology*, *558*(March 2018), 184–195. https://doi.org/10.1016/j.jhydrol.2018.01.027

Winton, R. S., Calamita, E., & Wehrli, B. (2019). Reviews and syntheses: Dams, water quality and tropical reservoir stratification. *Biogeosciences*, *16*(8), 1657–1671. https://doi.org/10.5194/bg-16-1657-2019